Published in final edited form as:
J Immunol. 2012 February 15; 188(4): 1647–1655. doi:10.4049/jimmunol.1103001.

OX40L and PD-L2 expression on inflammatory dendritic cells regulates CD4 T cell cytokine production in the lung during viral disease

Sarah E Wythe[*], **Jonathan S Dodd**[*], **Peter J Openshaw**[*], and **Jurgen Schwarze**[*,†]

[*]Center for Respiratory Infections, National Heart and Lung Institute, St. Mary's Campus, Imperial College London, UK.

[†]Child Life and Health, and Centre for Inflammation Research, Queen's Medical Research Institute, University of Edinburgh, 47 Little France Crescent, Edinburgh, EH16 4TJ, UK

Abstract

CD4-T-helper-cell (Th) differentiation is influenced by costimulatory molecules expressed on conventional dendritic cells (DCs) in regional lymph nodes and results in specific patterns of cytokine production. However, the function of costimulatory molecules on 'inflammatory' (CD11b+) DCs in the lung during recall responses is not fully understood, but important for development of novel interventions to limit immunopathological responses to infection. Using a mouse model in which vaccination with vaccinia virus vectors expressing the respiratory syncytial virus (RSV) fusion protein (rVVF) or attachment protein (rVVG) leads to type 1- or type 2-biased cytokine responses respectively upon RSV-challenge, we found expression of CD40 and OX40L on lung inflammatory DCs was higher in rVVF- than in rVVG-primed mice early after RSV-challenge, while the reverse was observed later in the response. Conversely, PD-L2 was higher in rVVG-primed mice throughout. Inflammatory DCs isolated at the resolution of inflammation revealed OX40L on type 1-biased DCs promoted IL-5, while on type 2-biased DCs enhanced IFNγ production by antigen-reactive Th cells. In contrast, PD-L2 promoted IFNγ production irrespective of conditions, suppressing IL-5 only if expressed on type 1-biased DCs. Thus, OX40L and PD-L2 expressed on DCs differentially regulate cytokine production during recall responses in the lung. Manipulation of these costimulatory pathways may provide a novel approach to controlling pulmonary inflammatory responses.

Introduction

Upon respiratory viral challenge, conventional lung dendritic cells (DCs) mature and migrate to the regional lymph nodes where they present antigen in the context of MHC to naïve antigen–specific T cells (1-3). During this period of activation, naïve CD4 T cells are educated to become T helper (Th)1, Th2, Th17, regulatory T cells (Treg) or remain part of a large uncommitted population (Th0) that can become polarized at a later stage (4). It now seems that polarization is reversible, and that both human and mouse Th1 and Th2 cells maintain flexibility and can respond to alternative polarizing conditions (5-7). These conditions consist of a combination of cytokines and costimulatory signals typically

Address for correspondence: Prof Jürgen Schwarze, MD, FRCPCH Child Life and Health, and Centre for Inflammation Research, Queen's Medical Research Institute, University of Edinburgh 47 Little France Crescent, Edinburgh, EH16 4TJ, UK jurgen.schwarze@ed.ac.uk Tel: +44 131 2426588; Fax: +44 131 2426554.
Current address: Sarah Wythe: MRC/Asthma UK Centre in Allergic Mechanisms of Asthma, King's College London, School of Medicine, Division of Asthma, Allergy & Lung Biology, 5th Floor, Tower Wing Guy's Hospital, London, SE1 9RT. sarah.wythe@kcl.ac.uk

Europe PMC Funders Author Manuscripts

provided by antigen presenting cells (APCs), in particular conventional DCs (5-7). In models of allergic airway inflammation, DCs have been shown to be required not only to initiate but also to maintain recall T cell responses (8).

Many costimulatory molecules expressed by DCs have been shown to be important in regulating T cells during both primary and recall responses. There is evidence that cytokine production by effector CD4 T cells is solely dependent on DC-derived costimulatory signals such as CD40 (9). However, naïve and effector T cells differ in the type of costimulation required for activation/reactivation. For example, CD80 and CD86 are critical for induction but not reactivation of Th2 cells in an ovalbumin (OVA)-driven mouse model of asthma (10). In contrast, OX40L is critical for reactivation of Th2 cells in this model (11).

Inflammatory monocytes are recruited to the lung during inflammation where they mature into CD11b+ (inflammatory) DCs (12). These cells have been shown to increase in numbers after primary respiratory syncytial virus (RSV) infection, associated with increased CD86 expression, which outlasted viral illness and peak inflammation (13). Recently inflammatory DCs have been shown to be important in the formation of tertiary lymphoid structures in the lung and optimal humoral immune responses after viral infection (14). However, the functional consequences of costimulatory molecule expression on inflammatory DCs for effector CD4 T cell cytokine production in type 1- and type 2-polarising environments in the lung have not been studied. In this study we hypothesized that inflammatory DCs provide a dominant signal in modulating antigen-specific recall responses of CD4 T cells. To address this hypothesis we used a well characterised mouse model of type 1- and type 2-biased responses to RSV infection. In this model, the only variable is the antigen used to sensitize prior to RSV challenge: immunization with recombinant vaccinia virus vectors expressing the RSV fusion protein (rVVF) or the RSV attachment protein (rVVG) leads to type 1- or type 2-biased responses respectively during subsequent RSV infection (15-16).

We found that lung DCs matured in type 1- or type 2-biased environments differed significantly in their expression of CD40, OX40L and PD-L2. These differences were most pronounced 10 days after RSV challenge, at which time viral replication had passed, airway cytokine levels had returned to baseline and the disease was resolving. However, DCs isolated from the lungs at this stage still biased T cell responses according to the environment from which they came in the absence of detectable IL-12p70 in the immediate environment. The costimulatory molecule OX40L promoted IFNγ production when expressed on DCs isolated from a type 2-biased environment and IL-5 when expressed on DCs isolated from a type 1-biased environment. In contrast, PD-L2 was Th1-enhancing irrespective of the environment from which the DC came. Our data suggest that OX40L and PD-L2 expression on DCs, at the time of isolation are functioning to restore the cytokine balance in the lung. Modulation of these pathways in the airways has the potential to alleviate viral induced immunopathology.

Materials and Methods

Mice and virus stocks

Eight week-old female BALB/c mice were purchased from Charles River Laboratories, UK. A DO11.10 mouse colony was established from breeding pairs donated by Professor Claire Lloyd and bred in-house. All mice were kept in specific pathogen-free conditions. RSV (A2 strain, grown on HEp2 cells following plaque purification); and recombinant vaccinia virus Western Reserve strain (rVV) expressing the RSV-fusion protein (F) or attachment protein (G) genes (or β-galactosidase (rVVβgal) as a control) in place of the thymidine kinase (*tk*) gene, were grown as previously described (17). All animal work was approved by the Home Office, London, UK.

Vaccination and RSV-infection

Under anaesthesia with isofluorane, mice were scarified on the rump and 3×10^6 pfu (in 10μl) rVVF, rVVG, or rVVβ-gal administered. In brief, the rumps of mice were shaved, and the skin decornified with an emery board. The viral inoculum was adsorbed to the decornified site, and the mice were observed until fully recovered. Two weeks later, these mice and naive controls were infected intranasally with 5×10^5 pfu (in 100μl) RSV or mock infected with HEp2 lysate, under anaesthesia with isofluorane, as described previously (15). Mice were weighed and monitored daily thereafter. At various time points post-challenge mice were culled by overdose of pentobarbitone (3mg, i.p.)

Cell and tissue recovery

Bronchoalveolar lavage (BAL) was performed as described (17) with 1ml of PBS. The BAL fluid (BALF) retrieved was centrifuged and the supernatant removed and stored at −80°C prior to analysis. BALF cells were resuspended in PBS/1% BSA /0.1% sodium azide in preparation for flow-cytometric analysis. Lungs were perfused with PBS via the heart prior to removal. They were then macerated and enzymatically digested by incubation with 0.1% collagenase solution for one hour. Cells were washed with PBS and single cell suspensions obtained by filtration. Red blood cells were lysed with ACK buffer. Live cells were enumerated by trypan blue exclusion using a haemocytometer.

Flow cytometric analysis of cell surface antigens

BALF, lung and splenic cells were resuspended in PBS/1% BSA /0.1% sodium azide. After blocking Fc-receptors with anti-CD16/32 antibodies (BD Biosciences, Oxford, UK), surface stains were performed by incubating cells for 30 mins at 4°C with the appropriate combinations of the following antibodies and isotype controls: anti-CD11c PE Cy5.5(N418), Hamster IgG PE Cy5.5(530-6) both from Caltag Laboratories (Burlingame, CA); anti-MHCII APC(M5/114.15.2), anti-ICOSL PE (HK5.3), anti-OX40L PE (RM134L), anti-PD-L1 PE (MIH5), anti-PD-L2 PE (122), Rat IgG2b APC (Eb149/10H5) all from ebioscience (San Diego, CA), and anti-CD40 PE (3/23), anti-CD80 PE (16-10A1), anti-CD86 PE (GL1), anti-CD11b FITC (M1/70), anti-B220 Cy (RA3-6B2), anti-CD3 Cy (154-2C11), anti-CD4 APC (RM4-5), OX40 FITC (OX-86) [AbD Serotec, Kidlington, UK], anti-CD40L FITC (MR1) [eBioscience, Hatfield, UK], anti-PD1 PE (J43), anti-MHCII FITC (2G9), Rat IgG2a $_\kappa$ FITC (R35-95), Rat IgG2b $_\kappa$ FITC (A95-1), Rat IgG2b $_\kappa$ PE (A95-1), Rat IgG2a $_\kappa$ PE (R35-95), Armenian hamster IgG2 $_\kappa$ PE (B81-3) all from BD Biosciences, unless the provider is indicated in brackets. Cells were washed and fixed for 15 minutes at 4°C with 4% formalin. Samples were analysed on a Cyan-9 (DAKO) flow cytometer. Eosinophils were identified as $B220^-CD3^-$ $MHCII^-CCR3^+$ cells that were lymphocytic in size (18).

Generation of antigen-reactive ‘effector’ CD4 T cells with an intermediate Th1/Th2 profile

BALB/c mice were injected intraperitoneally with 0.1μg of OVA peptide (Cambridge Research Biochemicals, Cambridge UK) adsorbed to alum (100μl) (Perbio Science UK Ltd, Cramlington, UK). After 7 days, spleens were removed and whole splenocyte populations were cultured in the presence of 17μg/ml OVA peptide (323-339) (19). CD4 positive cells were isolated 5 days later by positive immunomagnetic selection as described below.

Cell sorting

CD4 T cells were isolated from the spleens of DO11.10 or BALB/c mice, or from *in vitro* splenic cell cultures by first depleting the CD11c+ cells to remove CD4+ antigen presenting cells (APC). CD4 T cells were then isolated by positive selection with anti-CD4 MACS beads using an AutoMACS (Miltenyi, Bergisch-Gladbach, Germany). The purity of CD4 T cell populations was consistently above 90% (>97% when isolated from splenic cell culture)

(Supplementary Fig.2). DCs were isolated from the lungs of vaccinated BALB/c mice 10 days after RSV-challenge. Single cell suspensions pooled from 16 lungs per group. Fc receptors were blocked with anti-CD16/32 Abs (Fc block, BD Pharmingen) prior to enrichment of CD11c+ cells using anti-CD11c MACS beads. Lung DCs were isolated from CD11c-enriched populations by FACS collecting $CD11c^{+}$ $MHCII^{high}$ cells. The majority of these (>70%) expressed CD11b, while only a minority (<16%) expressed the macrophage marker F4/80. The purity of this population was consistently above 95%. Cell viability was consistently greater than 95% as assessed by trypan blue exclusion.

DC and alveolar macrophage morphology

Isolated DCs from primed and RSV-challenged mice, and alveolar macrophages from BALF of naive BALB/c mice were placed into chamber slides (1×10^5 per well) and stimulated overnight with LPS (10μg/ml) (Sigma-Aldrich Ltd, Dorset, UK) The cells were H&E-stained and visualised by phase microscopy. Cells were considered to be DCs if they exhibited dendrite formation (20).

Inflammatory DC co-cultures with naïve DO11.10 and 'effector' CD4 T cells by DCs

DCs isolated from lungs of rVVF- or rVVG-primed mice 10 days after RSV-challenge were pulsed with concentrations of OVA peptide (residues 323-339) ranging from 10-10,000nM or equivalent concentrations of an irrelevant peptide control (Amyloid Beta 25-35 (Cambridge Research Biochemicals, Cambridge, UK) for 1 hour at 37°C / 5%CO_2. CD4 T cells isolated from spleens of DO11.10 mice or splenic cell cultures ('effectors') were added to DCs at a ratio of 10:1 respectively. Cells were incubated at 37°C/5% CO_2 for 96 hours and concentrations of IFNγ, IL-4,IL-5 and IL-12p70 in culture supernatants determined by ELISA.

Functional antibody blockade of OX40L and PD-L2 on DCs

DCs isolated from rVVG- or rVVF-primed mice 10 days after RSV-challenge were incubated with 5μg/ml (determined by prior titration) of functional grade blocking anti-OX40L (RM134L) or anti-PD-L2 (Ty25) antibodies or the relevant isotype controls, $RatIgG2a_{\kappa}$, and RatIgG2b (ebioscience). Naive or 'effector' CD4 T cells were then cocultured with OVA-peptide-pulsed DCs for 96 hours. Concentrations of IFNγ, IL-4,IL-5 and IL-12p70 in the culture supernatants were determined by ELISA.

Cytokine ELISAs

The concentrations of IFNγ, IL-4 and IL-5 in BALF were determined using the following paired antibodies: IFNγ; purified (AN-18) and biotinylated (RA-6A2), IL-4; purified (BVD4-1D11) and biotinylated (BVD6-24G2), IL-5; purified (TRFK5) and biotinylated (TRFK4) respectively (BD Biosciences, Oxford, UK). TSLP and IL-12p70 levels were assessed using a DuoSet (R&D Systems, Abingdon, UK). 1) 96 well Maxisorp™ plates were coated with purified capture antibody (BD: 1:500 in sodium hydrogen carbonate buffer pH 9.6; R&D: 1:200 in PBS; pH 7.2) and incubated overnight at 4°C; 2) Following a blocking step with PBS/BSA (1% w/v) (2hrs RT), samples and standards were added in triplicate and incubated overnight at 4°C; 3) Biotinylated antibodies were diluted as for primary antibodies, but in PBT diluent [PBS/BSA(1%w/v)/Tween 20 (0.1% v/v)], and incubated for 1hr at RT; 4) Extravidin-HRP was diluted 1:1000 in PBT diluent, plates incubated for 30 mins at RT; 5) o-Phenylenediamine dihydrochloride substrate was added and plates observed for the colorimetric reaction; 6) The reaction was stopped using 1N H_2SO_4. Wells were washed in between steps 2-4 with PBS/Tween 20 (0.1% v/v). Optical density values were determined using a spectrophotometer (Molecular Devices) at 490nm reference wavelength. Cytokine concentrations were calculated from the standard curves.

Europe PMC Funders Author Manuscripts

The range for each standard curves were as follows: of IFNγ (4000-8pg/ml), IL-4 (2000-8pg/ml), IL-5 (2000-8pg/ml), IL-12p70 (2500-10pg/ml) and TSLP (1000-8pg/ml).

Statistical analysis

All statistical analysis was performed using GraphPad Prism 5.0 software (GraphPad, SanDiego, CA, USA). Students *t* test or Mann Whitney test were used to determine whether two groups differed significantly from each other for parametric or non-parametric data respectively. One-way analysis of variance (ANOVA) was used when comparing more than two groups. If the groups differed significantly a Tukey post-test was applied to determine where those differences lie. $P<0.05$ was considered significant.

Results

Memory responses elicit earlier weight loss than primary responses upon RSV challenge

Weight loss is a reliable marker of illness and lung pathology in this model, and is accelerated by prior sensitizing vaccination (15). After primary infection with RSV, mice began to lose weight on d5 post infection, with peak weight loss occurring at d8 p.c [Fig. 1(a)]. In comparison, uninfected and mock infected control mice did not lose weight over the same period of time. In contrast, mice previously vaccinated with rVVF or rVVG began to lose weight from d1 post RSV challenge (p.c) [Fig.1(b)], and weight loss peaked at d6 p.c, (two days earlier than in primary infection). Mice vaccinated with rVVβGal exhibited the same kinetic of weight loss upon RSV challenge as during primary infection.

Type 1 and 2 cytokine responses to RSV challenge after rVVF or rVVG priming

To confirm biased cytokine responses in primed mice, we measured the concentrations of IFNγ , IL-4, IL-5 [Fig.2(a-c)], IL-12p70 and the Th2-inducing epithelial-derived cytokine, thymic stromal lymphopoietin (TSLP) (21) [Fig.2(d)] in the BALF after RSV challenge. No IL-12p70 was detected in BALF in any of the groups over the duration of the response (data not depicted). In mice vaccinated with rVVβGal, IFNγ became detectable on d4, peaked on d7 and returned to baseline by d10 p.c. IFNγ responses measured in the BALF were accelerated and enhanced in mice primed with rVVF and rVVG; on d4 and 7 p.c., the concentration of IFNγ in the BALF was significantly greater in rVVF- than in rVVG-vaccinated mice ($p<0.01$) [Fig.2(a)]. By contrast, IL-4, which was detectable in both rVVF and rVVG, but not in rVVβGal vaccinated mice, was found at, significantly higher levels in rVVG-vaccinated mice on day 4 p.c. [Fig.2(b)]. Together these findings indicate type 1 bias after rVVF priming and type 2 bias after rVVG priming. IL-5 was detectable in all three groups. In rVVF- and rVVβGal IL-5 levels peaked on d7 p.c. at ~75pg/ml in rVVF- and <50pg/ml in rVVβGal-vaccinated mice. IL-5 levels in rVVG-vaccinated mice peaked earlier (d4 p.c.) and were significantly increased relative to other groups (~150pg/ml), again indicating type 2 bias [Fig.2(c)].

BALF TSLP levels were measured at 30-40 pg/ml prior to RSV challenge in all mice, probably representing basal production from the lung epithelia (22); [Fig.2(d)]. After RSV infection, TSLP fell steadily in both the rVVβGal and rVVF vaccinated groups to ~10pg/ml by d10 p.c. However, after an initial decline the concentration of TSLP in the BALF of rVVG vaccinated mice increased to 50pg/ml on d4 p.c. [Fig.2(d)].

To demonstrate a functional consequence of type 2 bias, eosinophil recruitment to the BALF was determined by flow cytometry at the peak of inflammation [Fig.2(e-f)]. On d7 p.c, eosinophils constituted 13% of total BALF cells ($23.7\pm4.8\times10^4$cells) in the rVVG-vaccinated mice compared to less than 3% ($4.7\pm0.7\times10^4$cells/ml) and 2% ($0.7\pm0.1\times10^4$cells/ml) respectively in mice primed with rVVF or rVVβGal [Fig.2(e-f)]. This confirmed a

functional type 2 immune response in rVVG-primed mice that was not detected in the other groups.

Increases in inflammatory DC numbers following RSV challenge are not affected by type 1- or type 2-biased environments

To examine whether priming with different antigens caused a change in the magnitude of the inflammatory DC ($MHCII^{hi}CD11c^{+}CD11b^{+}$) response, we enumerated lung inflammatory DCs during the course of RSV infection. The number of inflammatory DCs (23) increased ≥8 fold after infection, peaking at $1.2\text{-}1.6\times10^{6}$ cells/lung on d7 p.c. [Fig. 3]. Vaccination seemed to slightly delay the peak of DC numbers to d10 p.c. but did not significantly affect the absolute numbers of DCs at any time point.

DC costimulatory molecule expression differs between type 1- and type 2-biased environments

We next tested whether inflammatory DCs expressed a different repertoire of costimulatory molecules in different environments. The percentage of DCs expressing costimulatory molecules was generally greater in vaccinated compared to mock-vaccinated (rVVβGal) mice. Prior to RSV challenge, < 30% of DCs expressed the costimulatory molecules CD80/86, commonly associated with maturation (data not depicted); < 10% expressed CD40 [Fig.4(a)], < 5% OX40L [Fig.4(b)] and < 20% PD-L2 (Fig.4c). In contrast, >40% expressed ICOSL and >60% expressed PD-L1 (data not depicted). There were no significant differences in costimulatory molecule expression between the groups prior to RSV infection. After infection, the percentage of DCs expressing CD80/86 increased to 60%, and those expressing ICOSL and PD-L1 rose to 70% and 80% respectively by day 10 p.c. There were no significant differences between rVVF- and rVVG-vaccinated mice (data not depicted).

In contrast, CD40, OX40L, and PDL2 were differentially expressed following RSV challenge [Fig 4 and Supp Fig.1]. By d2 p.c CD40 expression rose to 36±2.7% of lung DCs in mice vaccinated with rVVF, significantly more than in the other two groups [Fig.4(a) and Supp Fig.1]. Expression then dropped to 15.6±1.6% of lung DCs by d7 p.c and remained at similar levels thereafter. This contrasted with rVVG-vaccinated mice where CD40 expression rose more slowly and reached at 25.0±3.2% on d7 p.c. At this time point there were significantly more CD40+ DCs in the lungs of rVVG-vaccinated mice ($p<0.01$) than in the other groups and this difference was maintained at d30 p.c.

There were similar kinetics of expression for OX40L [Fig.4(b) and Supp Fig.1] peaking on d2 p.c in rVVF-vaccinated mice followed by deceased expression, and a delayed peak expression on d10 p.c in rVVG-primed mice. The percentage of OX40L+ DCs also remained significantly higher in rVVG-vaccinated mice up to d30 p.c. In contrast, the percentage of PD-L2+ DCs was significantly higher in rVVG-vaccinated mice ($p<0.01$) at all time points assessed, peaking on d7 p.c at 70.0±3.4 of lung DCs in rVVG-vaccinated mice compared with at 40.0±0.4 in rVVF-primed mice [Fig.4(c) and Supp Fig.1].

We also measured the known ligands for these costimulatory molecules; CD40L, OX40 and PD1 on CD4 T cells in the lung (Supplementary Figure 4). CD40L [Supplementary figure 4(a)] and PD1 [Supplementary figure 4(b)] increased after RSV challenge peaking on day 7 with significantly more CD4 T cells expressing CD40L and PD1 in rVVG-compared to rVVF-primed mice ($p<0.001$). However, by day 10 p.c. both CD40L and PD1 were undetectable. In contrast, OX40 expression peaked on day 10 p.c. in both rVVG- and rVVF-vaccinated mice and there were no significant differences between the two groups at this time point [Supplementary figure 4(a)]. Interestingly, on day 30 p.c, CD40L and PD1, but

Europe PMC Funders Author Manuscripts

not OX40 were again expressed on CD4 T cells with significantly more CD4 T cells expressing CD40L and PD1 in rVVG- compared to rVVF-primed mice ($p<0.001$).

Isolated lung DCs from type 1- and type 2-biased environments are viable and induce biased cytokine responses in naïve and 'effector' CD4 T cells

Having shown that the immune environment in which inflammatory DCs mature, programs them to express a specific repertoire of costimulatory molecules, we investigated whether these DCs can regulate cytokine production by CD4 T cells. To specifically investigate the role of DC-expressed costimulatory molecules on CD4 T cells, we isolated viable, functional inflammatory DCs by sorting $MHCII^{hi}$, $CD11c^{+}$, $F4/80^{lo}$, $CD11b^{+}$ cells [Fig. 5(a)]; in these, viability was consistently >95% and sorted cells developed dendrites in response to LPS stimulation (not seen on alveolar macrophages under the same conditions; [Fig.5(b)]). Next, we assessed the ability of these DCs pulsed with OVA peptide to bias naïve and effector CD4 T cells. Naïve OVA-specific CD4 T cells were isolated from the spleens of DO11.10 mice [>91% pure; Supp Fig.2(a)&(b)]. DCs pulsed with an irrelevant peptide did not induce any cytokine production by CD4 T cells from DO11.10 mice [Fig. 5(c-e)], but OVA-peptide pulsed DCs from both rVVF- and rVVG-vaccinated mice induced IFNγ production by DO11.10 T cells. This was significantly increased if DCs were obtained from rVVF-primed mice [Fig.5(c)]. Conversely, DCs isolated from rVVG-vaccinated mice induced significantly greater levels of IL-5 [Fig.5(d)]. OVA-peptide pulsed DCs from both rVVF and rVVG induced IL-4 production from DO11.10 T cells [Fig.5(e)]. Subsequent co-culture experiments were carried out using an OVA peptide concentration of 10μM.

As inflammatory (CD11b+) DCs have been shown to form close contacts with effector CD4 T cells in organized lymphoid tissue in the lung after viral infection, we asked whether these DCs can influence cytokine production by non-naïve antigen-reactive cells. Antigen-reactive CD4 T cells with an intermediate Th1/Th2 profile were generated by culturing whole splenocyte populations from OVA-sensitized mice in the presence of OVA-peptide (24). CD4 T cells were then isolated by immunomagnetic separation [>97% pure; Supp Fig. 2(c&d)] and co-cultured with DCs. No cytokine production was detected in the presence of an irrelevant peptide (data not depicted). With OVA-peptide, IL-12p70 was below the level of detection (data not depicted), and only low concentrations of IL-4 [<10pg/ml; Fig.5(h)] could be measured. In contrast, IFNγ [Fig.5(f)] and IL-5 [Fig.5(g)] were detected, with a trend towards increased IFNγ production when CD4 T cells were co-cultured with rVVF-DCs, and increased IL-5 levels with rVVG-DC.

OX40 and PD1 are absent on naïve DO11.10 CD4 T cells, but up-regulated on antigen-activated CD4 T cells

Having shown differential upregulation of OX40L and PD-L2 on inflammatory lung DCs which cause biased cytokine responses in co-culture with naïve and antigen-activated CD4 T cells, we then assessed whether their known ligands were expressed on these T cells. Less than 1% of naïve CD4 T cells expressed OX40 (the true ligand for OX40L) and <2% expressed PD1 {the only identified ligand for PD-L2 [Supp Fig 3a(ii)]}. In contrast, approximately 10% of splenic CD4 T cells from OVA sensitized mice expressed OX40 and 2% expressed PD1. Following 5 days of antigen stimulation *in vitro*, the percentage of CD4 T cells expressing OX40 and PD1, individually or in combination, rose to >40% of the total CD4 T cell population [Supp Fig 3b(iv)]. In vivo, 10 days post RSV challenge, approximately 14×10^4 CD4 T cells in the lung expressed OX40 compared to approximately 3×10^4 cells at baseline thus confirming the possibility for OX40:OX40L interaction in both rVVF- and rVVG-primed mice in the lung at this time point. In contrast, PD1 (and CD40L) peaked at d7p.c. but were absent at d10p.c. (Supplementary figure 4).

PD-L2 promotes IFNγ production, but OX40L counter-regulates cytokine production by effector CD4 T cells

Using functional antibody blockade of OX40L and PD-L2 in these co-cultures, we then investigated how these differentially-expressed costimulatory molecules regulate cytokine production by CD4 T cells. In cocultures with DO11.10 CD4 T cells, which were stimulated with a full peptide dose response curve, no significant effects of OX40L- or PD-L2 blockade on cytokine production were observed (data not depicted). In co-cultures with effector CD4 T cells, blocking OX40L on rVVG-DCs significantly reduced IFNγ production [$p<0.05$; Fig.6a(ii)], but had no effect on IL-5 production [Fig.6b(ii)]. Conversely, blocking OX40L on rVVF-DCs did not affect IFN-γ [Fig.6a(i)], but significantly reduced IL-5 production [Fig.6b(i)]. In contrast blocking PD-L2 significantly reduced IFNγ concentrations irrespective of the DCs used to activate effector CD4 T cells [Fig.6c(i-ii)]. It also significantly enhanced IL-5 levels, but only in co-cultures with rVVF- but not rVVG-DCs [Fig.6d(i)]. IL-4 levels were not changed by blocking of either costimulatory molecule (data not depicted).

Discussion

Here we show that CD40, OX40L and PD-L2 expression on lung DCs differ both in timing and magnitude during type 1- and type 2-biased immune responses to RSV infection and that these molecules modulate cytokine production by effector but not naïve CD4 T cells. We confirm the previously reported role for PD-L2 in promoting IFNγ production, but show for the first time that OX40L counter-regulates ongoing cytokine production by effector CD4 T cells. This study highlights these two molecules as strong candidates for novel therapeutic targets to modulate CD4 T cell responses to respiratory pathogens, and potentially other infectious agents.

It is known that DCs play a critical role in both activation and reactivation of T cells and can deliver polarizing signals to T cells mediated by cytokines or costimulatory molecules. Of the costimulatory molecules we investigated, only CD40, OX40L and PD-L2 differed in their expression between the two environments. Ligation of CD40 has been shown to be critical for full activation and function of DCs, and has also been closely associated with the induction of Th1 responses through increasing IL-12p70 production (25-26). Although in this study CD40 expression was significantly increased in the type 1 environment on day 2 post-challenge, no IL-12p70 could be detected in the airways which may suggest a dominant role for costimulatory molecules in T cell polarization. In support of this, inflammatory DCs isolated from type 1-biased environments induced antigen-specific IFNγ responses in both naïve and effector CD4 T cells without detectable IL-12p70 in the immediate culture environment. Interestingly, effector T cells produced much less IFNγ than naïve T cells. As IL-5 levels were comparable, this was not due to the cells being Th2-biased. One possible explanation is that the reduction in IFNγ occurred due to repeated stimulation of the cells with peptide, alternatively it could be due to the reduced percentage of antigen-specific CD4 T cells in the effector T cell cocultures (27).

In order to delineate functional roles for OX40L and PD-L2 on lung DCs in viral inflammation, these molecules were blocked with antibodies during coculture with CD4 T cells. As CD40 is critical for DC activation, it would not constitute a good therapeutic target, so we focused on delineating the function of OX40L and PD-L2. Blocking these molecules had no effect on cytokine production by naïve CD4 T cells. We sought to explain this by assessing whether they expressed ligands for OX40L and PD-L2. OX40L binds exclusively to OX40 to exert its functional effects (28). In contrast, while the only identified ligand for PD-L2 is PD1, PD-L2 has been shown exert T cell stimulatory functions though binding an as yet unidentified ligand (29-30). We could detect OX40 and PD1 on effector but not naïve

T cells suggesting the lack of an effect of blocking OX40L and PD-L2 on DCs in cocultures with naïve CD4 T cells could be attributed to an absence of the ligands for these molecules. These results suggest that the factors other than those measured in this study are responsible for the observed bias in cytokine production from naïve CD4 T cells.

In contrast to naïve CD4 T cells, PD-L2 blockade on inflammatory DCs in coculture with effector CD4 T cells reduced IFNγ production irrespective of the environment from which the DC came and increased IL-5 production if blocked on DCs from a type 2 environment, indicating Th1-promoting effects of PD-L2. Our findings support those of other studies that show PD-L2 is upregulated on DCs in response to Th2 cytokines (31), but serves to down regulate them. For example, in a model of allergic airway inflammation, adoptive transfer of DCs activated through PD-L2 into pre-sensitized mice abrogated IL-4 production by T cells and completely protected the mice from allergic airway inflammation upon allergen challenge (32). Further, in a mouse model of leishmaniasis, in which host resistance is associated with Th1 responses and down-regulation of Th2 responses, PD-L2-deficiency resulted in exacerbated disease and increased parasite burden, indicative of an increased Th2 response (33).

In contrast to PD-L2, blockade of OX40L on DCs from a type 2 environment in co-culture with effector CD4 T cells reduced the production of IFNγ, while if blocked on DCs from a type 1 environment OX40L reduced IL-5 production. This may be explained by the findings that OX40-OX40L interactions can influence the immediate cytokine environment that can then influence Th differentiation. For example, while OX40 engagement preferentially leads to generation of Th2 cells which can be driven by autocrine IL-4 and related to enhanced calcium /NFATc signaling (21, 34-36), in the presence of IL-12 and IFNα, OX40:OX40L interactions lead to the induction of Th1 responses (21, 37-38). It should also be noted that reverse signals through OX40L result in the production of pro-inflammatory cytokines including IL-12, IL-6, IL-1, TNF and IFNα (39-41) from DCs, potentially through alterations in downstream signaling involving PKCβ2, c-Jun, and c-Fos (42).

We therefore speculate that in our system, modulation of inflammatory DC phenotype *in vivo* biases the DC to secrete different cytokines upon OX40L engagement which then influences the cytokine profile of the T cells following OX40:OX40L interaction. However, an alternative hypothesis could be that reverse signals from OX40L engagement result in cytokine secretion into the immunological synapse leading to differences in T cell cytokine production. Our data show that OX40:OX40L interaction on rVVF-primed DCs is promoting IL-5 production, while on rVVG-primed DCs it is promoting IFNγ. These data support our hypothesis that at the time of DC isolation, the DCs are functioning to restore the cytokine balance in the lung. To our knowledge our study is the first to describe such a regulatory role for OX40L. Expression of OX40 was also measured on lung CD4 T cells following RSV challenge. Expression of OX40 peaked on day 10p.c. in both rVVF and rVVG-primed mice confirming the possibility for OX40:OX40L engagement between CD4 T cells and inflammatory DCs in the lung. However, PD1 was absent at this time. The absence of PD1 *in vivo* does not contradict our hypothesis because, as previously mentioned, PD-L2 is most likely binding another ligand by which it exerts its T cell stimulatory functions.

Other studies have investigated the role of OX40:OX40L interactions in the induction of immune responses be they primary or memory (43-45). For example, induction of a primary Th2 response by TSLP-activated human monocyte-derived DCs was shown to occur in an OX40L-dependent manner (21). Moreover, in a mouse model of chronic *Leishmania major* infection, blocking OX40L on DCs reduced Th2 cytokines and anti-*L. major* IgG1 and IgE (46).

In contrast, in the present study we investigated the role of OX40L expression on DCs after viral clearance and at the beginning of resolution of pulmonary inflammation when inflammatory DC numbers were at their greatest. We show that in this phase of the response to RSV, OX40L expression on inflammatory DCs provides a negative feedback signal irrespective of the DCs' cytokine bias. The early expression of OX40L with CD40 on DCs in type 1 biased responses to RSV, taken together with their delayed expression in type 2 biased responses may indicate that during active viral infection, the function of inflammatory DCs is to stimulate anti-viral effector T cell functions, which can be suppressed or delayed by the presence of type 2 cytokines. However, after viral clearance, the function of these DCs changes from one of activation to one that aids resolution of inflammation and formation of optimal protective immunological memory. A recent study has shown that 10 days after viral challenge to the lung, inflammatory DCs are found in tertiary lymphoid organs (TLOs) in the lung in close contact with effector T and B cells (14). The interactions between inflammatory DCs and B cells within these TLOs have been shown to be essential for optimal anti-viral humoral responses. Although the precise function of inflammatory DCs within TLOs has not been studied, it has been suggested for a long time that DCs play an important role in terminating T cell responses both directly through interactions with negative regulators of T cell activation such as PD1 (47) and CTLA-4, as well as indirectly through induction of regulatory T cell responses (48). Our data support the hypothesis that the function of DCs and their costimulatory molecules is time and location dependent.

We therefore speculate that after prior antigenic exposure, and then airway pathogen challenge, antigen specific memory CD4 T cells are recruited to the lung and interact with DCs which serve to reactivate their effector function enabling them to secrete a previously determined cytokine profile. This initial wave of T cell responses biases the cytokine environment which in turn feeds back onto both resident and recruited inflammatory DCs resulting in upregulation of a specific repertoire of costimulatory molecules which further shapes anti-viral T cell responses. Once the virus has been cleared, inflammatory DCs become essential in the formation of TLOs where they are in close contact with effector T and B cells in the lung. At this stage we speculate that DC expression of OX40L (independently of the cytokine environment) and PD-L2 (in a dominant type 2 environment) are working with effector CD4 T cells to restore the cytokine balance in the lung. This neutralization of the dominant cytokine profile may inhibit ongoing inflammatory responses and prevent further cell recruitment, thereby promoting disease resolution.

It has not been previously demonstrated that costimulatory molecules expressed on DCs isolated from type 1- or type 2-biased environments can influence the cytokine production of activated naïve and effector CD4 T cells without the addition of polarizing cytokines into their immediate environment. These novel findings therefore demonstrate the central role of DC-expressed costimulatory ligands in governing CD4 T cell effector function. Since effector CD4 T cells exhibit functional plasticity in their ability to produce cytokines (5-7) our observations support the hypothesis that costimulatory molecules on DCs determine and modify the quality of T cell cytokine production in ongoing recall responses. This study highlights a new mechanism by which DCs control effector T cell responses during established inflammation in the lung. Thus, our study suggests that manipulation of OX40L and PD-L2 costimulatory pathways has the potential to reduce T-cell-dependent immunopathology. Such manipulation could provide the basis for novel immunomodulatory treatments not only for respiratory disease, but also for other inflammatory conditions where an imbalance of CD4-T-cell-derived cytokines is responsible.

Supplementary Material

Refer to Web version on PubMed Central for supplementary material.

Acknowledgments

The authors thank Dr Cecilia Johansson for critical review of this manuscript and Professor Brigitte Askonas for advice and guidance

Grant support: Wellcome Trust Senior Clinical Fellowship to JS (Grant no: 067454)

Abbreviations

RSV	Respiratory syncytial virus
rVV	recombinant vaccinia virus
β-gal	β-galactosidase
BALF	Bronchoalveolar lavage fluid

References

1. Crowe SR, Turner SJ, Miller SC, Roberts AD, Rappolo RA, Doherty PC, Ely KH, Woodland DL. Differential antigen presentation regulates the changing patterns of CD8+ T cell immunodominance in primary and secondary influenza virus infections. J Exp Med. 2003; 198:399–410. [PubMed: 12885871]
2. Legge KL, Braciale TJ. Accelerated migration of respiratory dendritic cells to the regional lymph nodes is limited to the early phase of pulmonary infection. Immunity. 2003; 18:265–277. [PubMed: 12594953]
3. Usherwood EJ, Hogg TL, Woodland DL. Enumeration of antigen-presenting cells in mice infected with Sendai virus. J Immunol. 1999; 162:3350–3355. [PubMed: 10092789]
4. Wang X, Mosmann T. In vivo priming of CD4 T cells that produce interleukin (IL)-2 but not IL-4 or interferon (IFN)-gamma, and can subsequently differentiate into IL-4- or IFN-gamma-secreting cells. J Exp Med. 2001; 194:1069–1080. [PubMed: 11602637]
5. Krawczyk CM, Shen H, Pearce EJ. Functional plasticity in memory T helper cell responses. J Immunol. 2007; 178:4080–4088. [PubMed: 17371962]
6. Lohning M, Hegazy AN, Pinschewer DD, Busse D, Lang KS, Hofer T, Radbruch A, Zinkernagel RM, Hengartner H. Long-lived virus-reactive memory T cells generated from purified cytokine-secreting T helper type 1 and type 2 effectors. J Exp Med. 2008; 205:53–61. [PubMed: 18195073]
7. Messi M, Giacchetto I, Nagata K, Lanzavecchia A, Natoli G, Sallusto F. Memory and flexibility of cytokine gene expression as separable properties of human T(H)1 and T(H)2 lymphocytes. Nat Immunol. 2003; 4:78–86. [PubMed: 12447360]
8. van Rijt LS, Jung S, Kleinjan A, Vos N, Willart M, Duez C, Hoogsteden HC, Lambrecht BN. In vivo depletion of lung CD11c+ dendritic cells during allergen challenge abrogates the characteristic features of asthma. J Exp Med. 2005; 201:981–991. [PubMed: 15781587]
9. MacLeod M, Kwakkenbos MJ, Crawford A, Brown S, Stockinger B, Schepers K, Schumacher T, Gray D. CD4 memory T cells survive and proliferate but fail to differentiate in the absence of CD40. J Exp Med. 2006; 203:897–906. [PubMed: 16549596]
10. van Rijt LS, Vos N, Willart M, Kleinjan A, Coyle AJ, Hoogsteden HC, Lambrecht BN. Essential role of dendritic cell CD80/CD86 costimulation in the induction, but not reactivation, of TH2 effector responses in a mouse model of asthma. J Allergy Clin Immunol. 2004; 114:166–173. [PubMed: 15241361]
11. Salek-Ardakani S, Song J, Halteman BS, Jember AG, Akiba H, Yagita H, Croft M. OX40 (CD134) controls memory T helper 2 cells that drive lung inflammation. J Exp Med. 2003; 198:315–324. [PubMed: 12860930]

12. Hammad H, Chieppa M, Perros F, Willart MA, Germain RN, Lambrecht BN. House dust mite allergen induces asthma via Toll-like receptor 4 triggering of airway structural cells. Nat Med. 2009; 15:410–416. [PubMed: 19330007]
13. Beyer M, Bartz H, Horner K, Doths S, Koerner-Rettberg C, Schwarze J. Sustained increases in numbers of pulmonary dendritic cells after respiratory syncytial virus infection. J Allergy Clin Immunol. 2004; 113:127–133. [PubMed: 14713917]
14. GeurtsvanKessel CH, Willart MA, Bergen IM, van Rijt LS, Muskens F, Elewaut D, Osterhaus AD, Hendriks R, Rimmelzwaan GF, Lambrecht BN. Dendritic cells are crucial for maintenance of tertiary lymphoid structures in the lung of influenza virus-infected mice. J Exp Med. 2009; 206:2339–2349. [PubMed: 19808255]
15. Dodd J, Riffault S, Kodituwakku JS, Hayday AC, Openshaw PJ. Pulmonary V gamma 4+ gamma delta T cells have proinflammatory and antiviral effects in viral lung disease. J Immunol. 2009; 182:1174–1181. [PubMed: 19124761]
16. Dodd JS, Lum E, Goulding J, Muir R, Van Snick J, Openshaw PJ. IL-9 regulates pathology during primary and memory responses to respiratory syncytial virus infection. J Immunol. 2009; 183:7006–7013. [PubMed: 19915054]
17. Openshaw PJ, Clarke SL, Record FM. Pulmonary eosinophilic response to respiratory syncytial virus infection in mice sensitized to the major surface glycoprotein G. Int Immunol. 1992; 4:493–500. [PubMed: 1591217]
18. van Rijt LS, Kuipers H, Vos N, Hijdra D, Hoogsteden HC, Lambrecht BN. A rapid flow cytometric method for determining the cellular composition of bronchoalveolar lavage fluid cells in mouse models of asthma. J Immunol Methods. 2004; 288:111–121. [PubMed: 15183090]
19. Mattes J, Yang M, Siqueira A, Clark K, MacKenzie J, McKenzie AN, Webb DC, Matthaei KI, Foster PS. IL-13 induces airways hyperreactivity independently of the IL-4R alpha chain in the allergic lung. J Immunol. 2001; 167:1683–1692. [PubMed: 11466392]
20. Grayson MH, Cheung D, Rohlfing MM, Kitchens R, Spiegel DE, Tucker J, Battaile JT, Alevy Y, Yan L, Agapov E, Kim EY, Holtzman MJ. Induction of high-affinity IgE receptor on lung dendritic cells during viral infection leads to mucous cell metaplasia. J Exp Med. 2007; 204:2759–2769. [PubMed: 17954569]
21. Ito T, Wang YH, Duramad O, Hori T, Delespesse GJ, Watanabe N, Qin FX, Yao Z, Cao W, Liu YJ. TSLP-activated dendritic cells induce an inflammatory T helper type 2 cell response through OX40 ligand. J Exp Med. 2005; 202:1213–1223. [PubMed: 16275760]
22. Soumelis V, Reche PA, Kanzler H, Yuan W, Edward G, Homey B, Gilliet M, Ho S, Antonenko S, Lauerma A, Smith K, Gorman D, Zurawski S, Abrams J, Menon S, McClanahan T, de Waal-Malefyt Rd R, Bazan F, Kastelein RA, Liu YJ. Human epithelial cells trigger dendritic cell mediated allergic inflammation by producing TSLP. Nat Immunol. 2002; 3:673–680. [PubMed: 12055625]
23. Smit JJ, Rudd BD, Lukacs NW. Plasmacytoid dendritic cells inhibit pulmonary immunopathology and promote clearance of respiratory syncytial virus. J Exp Med. 2006; 203:1153–1159. [PubMed: 16682497]
24. Kearley J, Barker JE, Robinson DS, Lloyd CM. Resolution of airway inflammation and hyperreactivity after in vivo transfer of CD4+CD25+ regulatory T cells is interleukin 10 dependent. J Exp Med. 2005; 202:1539–1547. [PubMed: 16314435]
25. Macatonia SE, Hosken NA, Litton M, Vieira P, Hsieh CS, Culpepper JA, Wysocka M, Trinchieri G, Murphy KM, O'Garra A. Dendritic cells produce IL-12 and direct the development of Th1 cells from naive CD4+ T cells. J Immunol. 1995; 154:5071–5079. [PubMed: 7730613]
26. Stuber E, Strober W, Neurath M. Blocking the CD40L-CD40 interaction in vivo specifically prevents the priming of T helper 1 cells through the inhibition of interleukin 12 secretion. J Exp Med. 1996; 183:693–698. [PubMed: 8627184]
27. Gett AV, Sallusto F, Lanzavecchia A, Geginat J. T cell fitness determined by signal strength. Nat Immunol. 2003; 4:355–360. [PubMed: 12640450]
28. Croft M. Control of immunity by the TNFR-related molecule OX40 (CD134). Annu Rev Immunol. 2010; 28:57–78. [PubMed: 20307208]

29. Liu X, Gao JX, Wen J, Yin L, Li O, Zuo T, Gajewski TF, Fu YX, Zheng P, Liu Y. B7DC/PDL2 promotes tumor immunity by a PD-1-independent mechanism. J Exp Med. 2003; 197:1721–1730. [PubMed: 12810690]
30. Shin T, Kennedy G, Gorski K, Tsuchiya H, Koseki H, Azuma M, Yagita H, Chen L, Powell J, Pardoll D, Housseau F. Cooperative B7-1/2 (CD80/CD86) and B7-DC costimulation of CD4+ T cells independent of the PD-1 receptor. J Exp Med. 2003; 198:31–38. [PubMed: 12847135]
31. Loke P, Allison JP. PD-L1 and PD-L2 are differentially regulated by Th1 and Th2 cells. Proc Natl Acad Sci U S A. 2003; 100:5336–5341. [PubMed: 12697896]
32. Liang SC, Greenwald RJ, Latchman YE, Rosas L, Satoskar A, Freeman GJ, Sharpe AH. PD-L1 and PD-L2 have distinct roles in regulating host immunity to cutaneous leishmaniasis. Eur J Immunol. 2006; 36:58–64. [PubMed: 16358363]
33. Matsumoto K, Inoue H, Nakano T, Tsuda M, Yoshiura Y, Fukuyama S, Tsushima F, Hoshino T, Aizawa H, Akiba H, Pardoll D, Hara N, Yagita H, Azuma M, Nakanishi Y. B7-DC regulates asthmatic response by an IFN-gamma-dependent mechanism. J Immunol. 2004; 172:2530–2541. [PubMed: 14764726]
34. Flynn S, Toellner KM, Raykundalia C, Goodall M, Lane P. CD4 T cell cytokine differentiation: the B cell activation molecule, OX40 ligand, instructs CD4 T cells to express interleukin 4 and upregulates expression of the chemokine receptor, Blr-1. J Exp Med. 1998; 188:297–304. [PubMed: 9670042]
35. Ohshima Y, Yang LP, Uchiyama T, Tanaka Y, Baum P, Sergerie M, Hermann P, Delespesse G. OX40 costimulation enhances interleukin-4 (IL-4) expression at priming and promotes the differentiation of naive human CD4(+) T cells into high IL-4-producing effectors. Blood. 1998; 92:3338–3345. [PubMed: 9787171]
36. So T, Song J, Sugie K, Altman A, Croft M. Signals from OX40 regulate nuclear factor of activated T cells c1 and T cell helper 2 lineage commitment. Proc Natl Acad Sci U S A. 2006; 103:3740–3745. [PubMed: 16501042]
37. De Smedt T, Smith J, Baum P, Fanslow W, Butz E, Maliszewski C. Ox40 costimulation enhances the development of T cell responses induced by dendritic cells in vivo. J Immunol. 2002; 168:661–670. [PubMed: 11777959]
38. Ito T, Amakawa R, Inaba M, Hori T, Ota M, Nakamura K, Takebayashi M, Miyaji M, Yoshimura T, Inaba K, Fukuhara S. Plasmacytoid dendritic cells regulate Th cell responses through OX40 ligand and type I IFNs. J Immunol. 2004; 172:4253–4259. [PubMed: 15034038]
39. Burgess JK, Carlin S, Pack RA, Arndt GM, Au WW, Johnson PR, Black JL, Hunt NH. Detection and characterization of OX40 ligand expression in human airway smooth muscle cells: a possible role in asthma? J Allergy Clin Immunol. 2004; 113:683–689. [PubMed: 15100674]
40. Diana J, Griseri T, Lagaye S, Beaudoin L, Autrusseau E, Gautron AS, Tomkiewicz C, Herbelin A, Barouki R, von Herrath M, Dalod M, Lehuen A. NKT cell-plasmacytoid dendritic cell cooperation via OX40 controls viral infection in a tissue-specific manner. Immunity. 2009; 30:289–299. [PubMed: 19217323]
41. Ohshima Y, Tanaka Y, Tozawa H, Takahashi Y, Maliszewski C, Delespesse G. Expression and function of OX40 ligand on human dendritic cells. J Immunol. 1997; 159:3838–3848. [PubMed: 9378971]
42. Matsumura Y, Hori T, Kawamata S, Imura A, Uchiyama T. Intracellular signaling of gp34, the OX40 ligand: induction of c-jun and c-fos mRNA expression through gp34 upon binding of its receptor, OX40. J Immunol. 1999; 163:3007–3011. [PubMed: 10477563]
43. Humphreys IR, Walzl G, Edwards L, Rae A, Hill S, Hussell T. A critical role for OX40 in T cell-mediated immunopathology during lung viral infection. J Exp Med. 2003; 198:1237–1242. [PubMed: 14568982]
44. Jember AG, Zuberi R, Liu FT, Croft M. Development of allergic inflammation in a murine model of asthma is dependent on the costimulatory receptor OX40. J Exp Med. 2001; 193:387–392. [PubMed: 11157058]
45. Tanaka H, Demeure CE, Rubio M, Delespesse G, Sarfati M. Human monocyte-derived dendritic cells induce naive T cell differentiation into T helper cell type 2 (Th2) or Th1/Th2 effectors. Role of stimulator/responder ratio. J Exp Med. 2000; 192:405–412. [PubMed: 10934228]

46. Akiba H, Miyahira Y, Atsuta M, Takeda K, Nohara C, Futagawa T, Matsuda H, Aoki T, Yagita H, Okumura K. Critical contribution of OX40 ligand to T helper cell type 2 differentiation in experimental leishmaniasis. J Exp Med. 2000; 191:375–380. [PubMed: 10637281]

47. Freeman GJ, Long AJ, Iwai Y, Bourque K, Chernova T, Nishimura H, Fitz LJ, Malenkovich N, Okazaki T, Byrne MC, Horton HF, Fouser L, Carter L, Ling V, Bowman MR, Carreno BM, Collins M, Wood CR, Honjo T. Engagement of the PD-1 immunoinhibitory receptor by a novel B7 family member leads to negative regulation of lymphocyte activation. J Exp Med. 2000; 192:1027–1034. [PubMed: 11015443]

48. Grohmann U, Puccetti P. CTLA-4, T helper lymphocytes and dendritic cells: an internal perspective of T-cell homeostasis. Trends Mol Med. 2003; 9:133–135. [PubMed: 12727137]

Europe PMC Funders Author Manuscripts

Europe PMC Funders Author Manuscripts

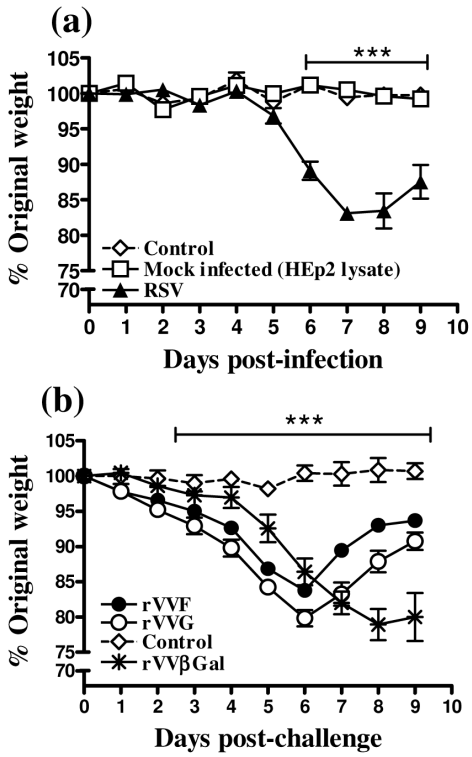

Figure 1. Memory responses elicit earlier weight loss than primary responses upon RSV challenge

(a) BALB/c mice were uninfected (control), or challenged intranasally with RSV or Hep2 lysate (Mock infection) or (b) were either unvaccinated and uninfected (Control) or vaccinated by scarification of the rump with rVVF, rVVG or rVVβGal and challenged with RSV intranasally 14 days later. All mice were weighed daily after RSV-challenge. These graphs are representative of 5 independent experiments ($n \geq 5$ per group) and show means ± SD. ANOVA (Tukey post test) result: (a) ***: $p<0.001$ for RSV versus control and Mock infected and (b) rVVF and rVVG versus control.

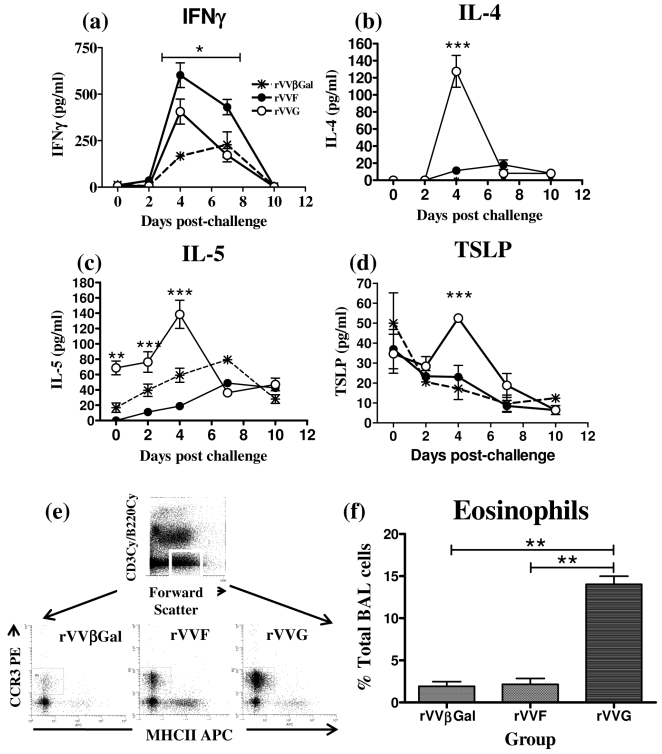

Figure 2. Type 1- and 2-biased responses to RSV challenge after rVVF or rVVG priming

BALB/c mice were vaccinated with rVVF, rVVG or rVVβGal. 14 days later mice were challenged with RSV intranasally. At various time points post-challenge mice were sacrificed and BALF harvested. BALF concentrations of (a) IFN-γ, (b) IL-4, (c) IL-5, and (d) TSLP were determined by ELISA. (e) BAL eosinophilia was determined by flow cytometry. Top panel: BALF granulocytes: forward scatter 360-760/B220cy^{-}/CD3cy^{-}, Lower panel: eosinophils: CD3^{-}B220^{-} MHCII^{-}CCR3^{+}. (f) Eosinophils as percentage of total BALF cells. The graphs are representative of three independent experiments (n ≥ 5 per group) and show means ± SD (a-e). ANOVA (Tukey post test) result: rVVF vs rVVG * = $p<0.05$, ** = $p< 0.01$, *** = $p<0.001$.

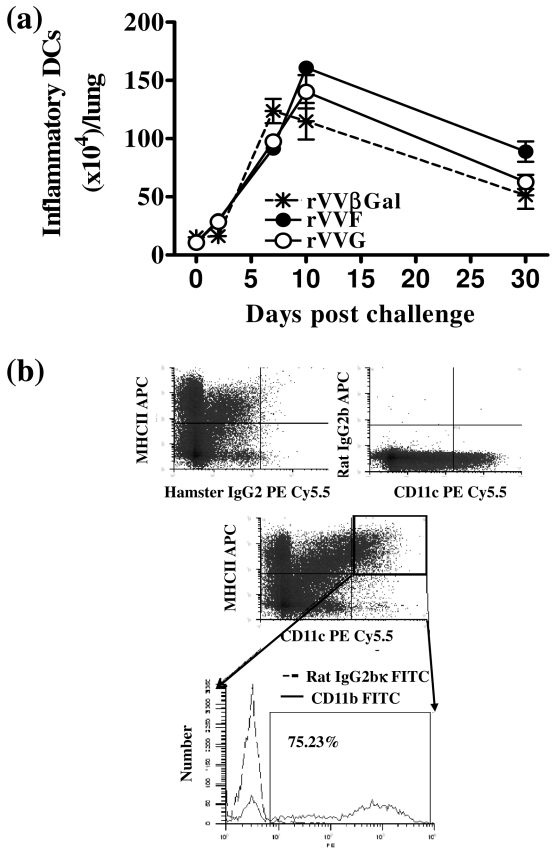

Figure 3. Inflammatory DC number in the lungs is not affected by type 1- or type 2-biased environments

BALB/c mice were vaccinated by scarification of the rump with rVVF, rVVG or rVVβGal and challenged with RSV. (a) On days 0, 2, 7, 10 and 30 p.c. mice were sacrificed and the number of inflammatory DCs in the lung determined. (b) Inflammatory DCs were defined as $CD11c^{+}$, $MHCII^{hi}$ and CD11b+. The graph is representative of two independent experiments ($n \geq 5$ per group) and show means ± SD.

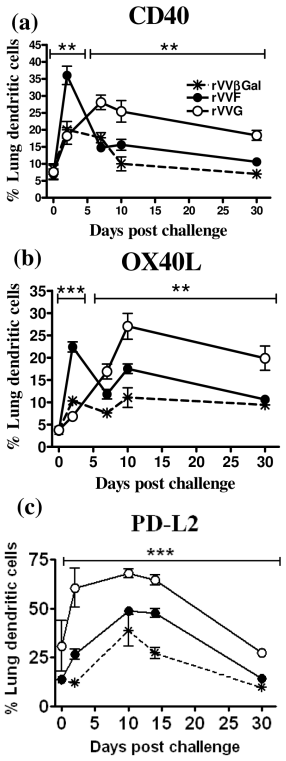

Figure 4. DC costimulatory molecule expression differs between type 1- and type 2-biased environments

BALB/c mice were vaccinated by scarification of the rump with rVVF, rVVG or rVVβGal and challenged with RSV. On days 0, 2, 7, 10 and 30 post challenge mice were sacrificed and the lungs harvested. The percentage of inflammatory DCs ($CD11c^{+}$ $MHCII^{hi}$ $CD11b^{+}$) in the lung expressing (a) CD40, (b) OX40L, and (c) PD-L2 were determined by flow cytometry. Representative dot plots are shown in Supplementary Figure 1. The graphs are representative of two independent experiments ($n \geq 5$ per group) and show means ± SD. ANOVA (Tukey post test) result: rVVF vs rVVG, ** = $p < 0.01$, *** = $p < 0.001$).

Europe PMC Funders Author Manuscripts

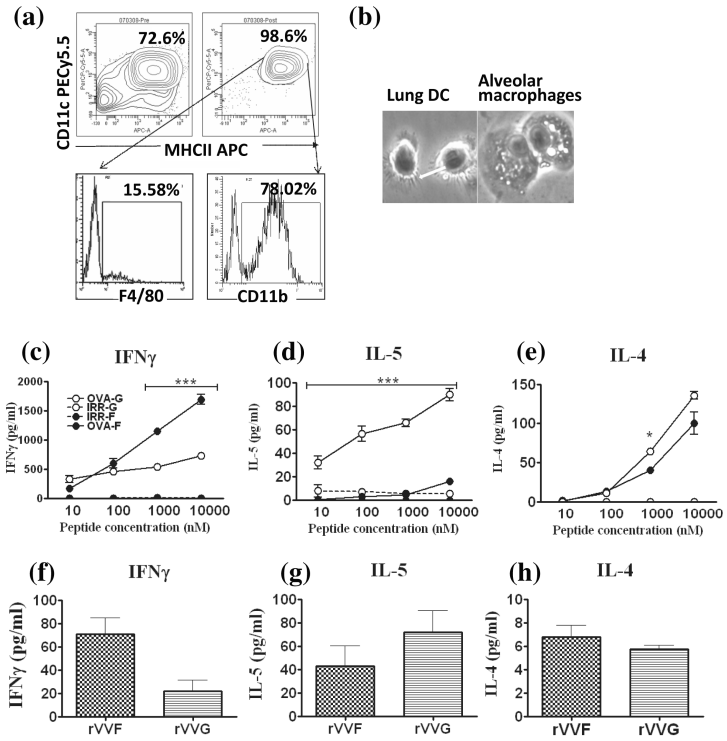

Figure 5. Isolated lung DCs from type 1- and type 2- biased environments are viable and induce polarized cytokine responses in naïve and effector CD4 T cells

BALB/c mice were vaccinated by scarification of the rump with rVVF or rVVG and challenged with RSV. On day 10 post-challenge mice were sacrificed and lungs harvested. Cells were pooled from the mice within each group and (a) DCs isolated from a CD11c enriched population by FACS sorting of $CD11c^{+}MHCII^{hi}$ cells. Top panel: CD11c enriched cells pre-FACS sorting (left) and post-FACS sorting (right). Lower panel: Expression of F4/80 on FACS-sorted cells (left) and expression of CD11b on FACS-sorted cells (right). (b) Isolated lung DCs and macrophages obtained from the BALF of naïve mice were cultured in the presence of LPS for 24 h and then H&E stained and imaged under phase microscopy at a magnification of x40. The arrow highlights dendrite formation. Naïve CD4 T cells were isolated from the spleens of DO11.10 mice (Supplementary Figure 2). 1×10^4 DCs per well were pulsed for one hour with increasing concentrations of OVA peptide (323-339) or an irrelevant peptide control (amyloid beta (residues 25-35) and then cocultured with 1×10^5 T cells per well for 96 hours. The supernatants were assayed for (c) IFN-γ, (d) IL-5, and (e) IL-4. 1×10^5 effector CD4 T cells were cocultured with 1×10^4 DCs pulsed with OVA peptide or an irrelevant peptide control (10μM) for 96 hours. The supernatants were assayed for (f) IFN-γ, (g) IL-5, and (h) IL-4. The graphs are representative of five independent experiments and show means ± SD (c-e). ANOVA (Tukey post test) result: OVA peptide –pulsed-rVVF DCs vs –rVVG DCs, * = $p < 0.05$, ** = $p < 0.01$, *** = $p<0.001$).

Europe PMC Funders Author Manuscripts

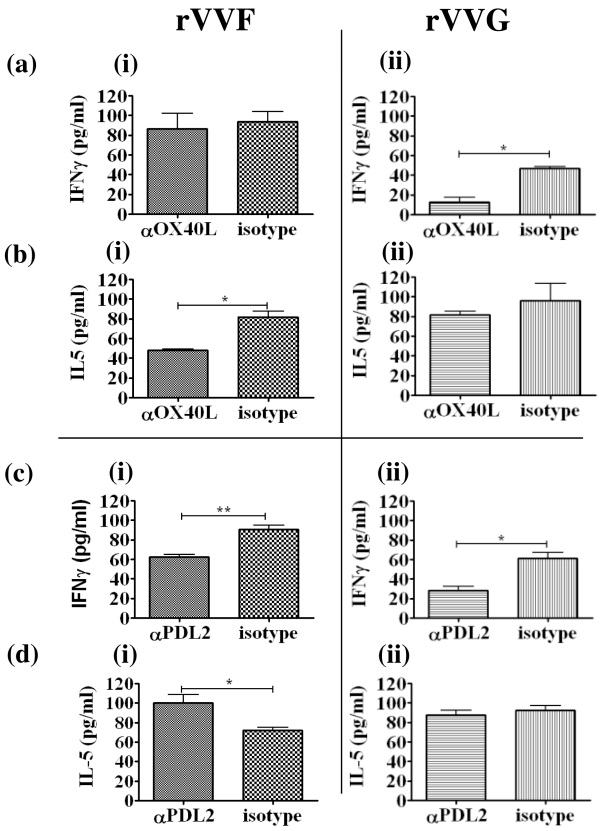

Figure 6. Cytokine production by effector CD4 T cells is differentially regulated by OX40L and PD-L2 expression on type 1- and type 2-biased inflammatory DCs

BALB/c mice were vaccinated by scarification of the rump with rVVF or rVVG and challenged with RSV. On day 10 post-challenge mice were sacrificed and lungs harvested. Cells were pooled from the mice with in each group and DCs isolated. 1×10^4 DCs per well from rVVF- (i) or rVVG- (ii) primed mice were pulsed for one hour with 10μM OVA peptide (323-339) and cocultured with 10^5 effector CD4 T cells per well for 96 hours in the presence of anti-OX40L (a, b) or anti-PD-L2 (c, d) or the relevant isotype controls. (a, c) IFN-γ and (b, d) IL-5 concentrations were determined by ELISA. The graphs are representative of two independent experiments and show means ± SD. Student *t*-test result * = $p < 0.05$, ** = $p<0.01$).